Low Complexity Image Compression Algorithm for Wireless Channel

Awad Khuzaim Al-Asmari

King Saud University, College of Engineering,
Electrical Engineering Department,
P. O. Box 800, Riyadh 11421
Saudi Arabia, E-mail: akasmari@ksu.edu.sa

Abstract. Pyramid coding with absolute moment block truncation coding (PC-AMBTC) technique is proposed for wireless image communication. The digital European cordless telecommunications (DECT) system is used as wireless communication environment. The impact of Channel fading on the PC-AMBTC technique is investigated and its performance is compared with other algorithms. The image is decomposed into two images (decimated image and the difference image). The AMBTC is used for the decimated image and a modified geometric vector quantization (MGVQ) is used for the difference image. Since most of the signal power and information is located in the low frequency band of the image, special attention is given to this band to protect its information from Channel fading errors. Simulation results show that the proposed technique is very robust to Channel fading errors. It is found that the performance of PC-AMBTC algorithm is better than the existing algorithms at the same bit rate.

Introduction

Image data compression is crucial for transmission of images over wireless Channels. The wireless communication radio suffers from burst error in which a large number of consecutive bits are lost or corrupted by the Channel fading effect [1-3]. Typically, the bit error rate (BER) in wireless Channel ranges from 10^{-1} to 10^{-6}, which may not be acceptable for transmitting compressed images, using traditional compression schemes such as JPEG. The JPEG standard for lossy image compression using discrete cosine transform (DCT) is not very flexible for progressive transmission of images [4-5]. Therefore, it is desirable to design a robust image coding technique, which has a high compression ratio and produces acceptable image quality over a fading Channel. The advent of hierarchical Pyramid schemes for coding has enabled such transmission to be achieved in a much more logical manner. Subband coding and Pyramid coding are the two candidates for progressive transmission [6].

Proposed algorithm

Recent works on digital image transmission over wireless Channels have investigated image transmission in the IS-54 environment and achieved compression rates varying from 0.25 bit per pixel (bpp) to 0.35 bpp with image quality varying from a very good coarser approximation to a near original quality image [7]-[8]. In the DECT environment two studies have been investigated with a transmission rate in the range of 0.73 bpp to 0.69 bpp [9]-[10] for the standard image 'Lena'. The proposed algorithm scheme combines the high quality Pyramid decomposition technique with a very low complexity encoder such as AMBTC and MGVQ algorithms. This hybrid image coding approach helps in achieving lower bit rates while keeping good visual quality of the reconstructed image.

Pyramid coding (PC) has been found to be a useful tool in many image-processing applications. Pyramid coding has less quantization noise than subband coding. It has been shown that Pyramid coding with three layers has a lower reconstruction error power spectrum than subband coding with three stages [6]. The Pyramid coding structure contains a lowpass FIR filter having a cutoff frequency $\pi/4$ that performs N levels partitioning. A lowpass analysis filter $h_0(n_1, n_2)$ is used to filter the image and obtain the baseband signal. Since most of the signal power and information is located in the low frequency band of the image (decimated image), special attention should be given to this band to protect its information from Channel fading errors.

In this paper, Pyramid coding (PC) with one-level for image decomposition will be adapted, where the baseband (decimated image) is encoded by absolute moment block truncation coding (AMBTC) and the high band is encoded by the modified geometric vector quantization (MGVQ).

The paper is organized as follows. The digital European cordless telecommunication (DECT) and its characteristic regarding the error Channel are discussed in section 2. In section 3, the PC-AMBTC algorithm is described. The Modified GVQ for the difference image is presented in section 4. The simulation results are given in section 5. The performance evaluation is given in section 6. Finally, the conclusions and future research are given in section 7.

Digital European Cordless Telecommunication

Cordless technology, in contrast to cellular radio such as global system for mobile communications (GSM), digital European cordless telecommunication (DECT) is a Pan-European standard developed by the European committee of posts and telegraphs. The purpose of DECT is to provide Europe with an advanced cordless communication system that will serve variety of needs at end of the twentieth century. While the range of target applications is similar to that of second generation cordless telephone CT2, the initial

deployment of DECT technology will be in a multicell business environment, rather than the single-cell telepoint of CT2. More than the other second generation system, DECT technology will make it possible for users with wireless terminals to gain access to the features of the emerging fixed ISDN public network [11]-[12].

A. Characteristics of DECT

The Carriers are separated by 1.728 Mhz and carry 12 Channels in a TDMA format. DECT employs time division duplex (TDD), so that the information moves in both directions over the same carrier. As shown in Fig. 1, the frame duration is 10 ms, with 5 ms for portable-to-fixed station transmission and 5 ms for fixed-to-portable. The transmitter assembles information in signal bursts which it transmits in slots of duration $5/12 = 0.417$ ms with 480 bits per slot (including a 64-bit guard time). The total bit rate is 1.152 Mb/s, the highest by far of any of second generation system, each slot contains 64 bits for system control (C-Channel) and 320 bits for user information (I-Channel). Thus, the raw data for C-Channel is 6.4 Kb/s. The modulation technique of DECT is Gaussian minimum shift keying (GMSK). The bandwidth efficiency is 0.67 b/s/Hz [7].
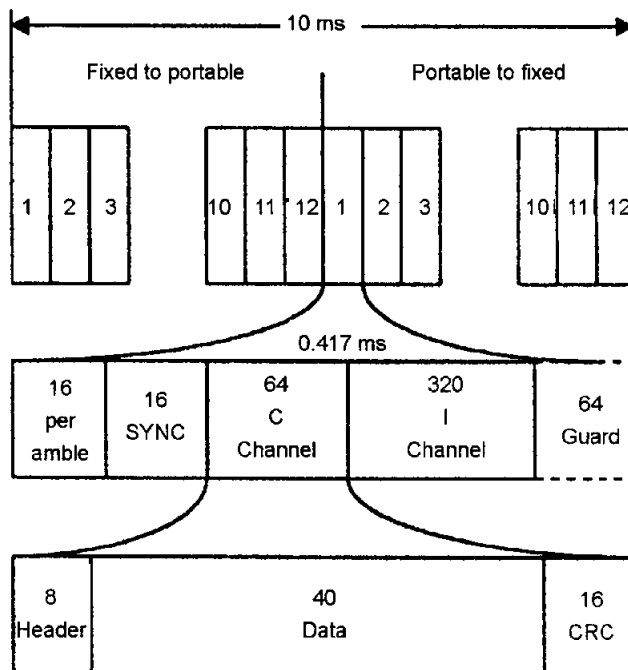

Fig. 1. The DECT characteristics.

The DECT relies on error detection and retransmission for accurate delivery of control information, and every 64 bits control word contains 16 parity check bits in addition to the 48-bit payload. The maximum information throughput of the DECT control Channel is 4.8 kb/s. With each control word contained in a signal frame, the average delay is 5 ms. Among the second generation system, the DECT control Channel has the best throughput and delay performance [12]-[13]. The DECT design is more adaptable to advanced information services such as wireless Internet and videophone. Also, the DECT system can be used for wireless Intranet inside a building or inside a big establishment instead of wire connection through the hard walls.

B. Channel error characteristics of the DECT system
To evaluate the Channel errors, three factors are considered:

I -The bit error rate (BER).
II -The average burst error length (ABER).
III -The mean burst error (MBE) time.

In any wireless network, a common feature is the fading effect. This fading effect is due to multi-path propagation of the signal and can cause burst errors during transmission. In the following subsections, BER and ABEL are calculated for the GMSK modulation scheme, which is the modulation scheme used in the DECT system [9].

I. BER performance of DECT
The measured static BER performance in the non-fading environment can be approximated [14] as:

$$p_c \cong \frac{1}{2} \text{erfc}(\sqrt{\alpha\gamma}\ ) \tag{1}$$

where erfc (x) is the complementary error function given by

$$\text{erfc}(x) = \frac{2}{\sqrt{x}} \int_x^\infty \exp(-u^2)\ du \tag{2}$$

α is a constant parameter and γ is the received Channel signal -to- noise ratio (SNR).

The relative bandwidth of the Gaussian filter (BT) in the DECT system is 0.5 (bT = 0.5). Typically, α is in the range of 0.68 (for GMSK with bT = 0.25) and 0.85 (for simple MSK (bT $\rightarrow\infty$)) [14].

In the practical V/UHF land mobile radio environment, signal transmission between a fixed base station and a moving vehicle is usually performed via random multiple

propagation routes. Consequently, fast and deep multi-path fading can generally be treated by the well-known Rayleigh fading model [9],[14].

In particular, when a quasi-stationary slow Rayleigh fading model is assumed, dynamic BER performance is given by

$$P_e(\Gamma) = \int_0^\infty P_e(\gamma)P(\gamma)d\gamma \tag{3}$$

where Γ is the average Channel SNR and $p(\gamma)$ is the probability density function (pdf) of γ given by

$$P(\gamma) = \frac{1}{\Gamma}\exp\left(\frac{-\gamma}{\Gamma}\right) \tag{4}$$

by substitution of equation (4), the BER for DECT system using GMSK modulation is given by:

$$p_e(\Gamma) \cong \frac{1}{2}\left(1 - \sqrt{\frac{\alpha\ \Gamma}{\alpha\ \Gamma + 1}}\right) \cong \frac{1}{4\alpha\ \Gamma} \tag{5}$$

However, the dynamic BER performance in the fast Rayleigh fading environment, where the temporal variation effect of the fading be neglected, has not yet been theoretically estimated because the tracking performance of the carrier recovery circuit in such environment cannot be analyzed [9].

II. Average burst error length

The average value of burst error length (ABEL) is estimated as follows. For simplicity it is assumed that the error rate property is approximated by rectangular characteristics [15], that is

$$P(\gamma) = \begin{cases} 1/2 & \gamma < T \\ 0 & \gamma \geq T \end{cases} \tag{6}$$

where T is the threshold level for detection.

Then, the BER in the Rayleigh fading is given by:

$$\overline{P}_e = \int_0^T \frac{1}{2\Gamma} \exp\left(\frac{-\gamma}{\Gamma}\right) d\gamma = \frac{\left\{1 - \exp\left(\frac{-T}{\Gamma}\right)\right\}}{2} \tag{7}$$

From equation (5) and (7), the threshold T can be calculated by setting $P_e(T) = \overline{P}_e(T)$. Then, T is determined as

$$T = -\Gamma \ln\left(\frac{2\alpha\ \Gamma - 1}{2\alpha\ \Gamma}\right) \cong \frac{1}{2\alpha} \qquad (\Gamma) >> 1 \tag{8}$$

However, if Γ is less than T, then the average fading duration is given as [15]:

$$S(T) = \frac{\{\exp(T/\Gamma) - 1\}}{f_d \sqrt{(2\pi T)/\Gamma}} \tag{9}$$

where f_d denotes the fading rate, therefore, the ABEL denoted by N_B [15] is deduced to be

$$N_B = \frac{S(T)}{T_0} = \left[2\alpha\ \Gamma f_d\ T_0 \sqrt{2\pi \ln\left(1 + 1/(2\alpha\ \Gamma)\right)}\right]^{-1} \tag{10}$$

where $T_0 = 1/f_b$ and f_b is the transmission rate.

III. Estimation of channel error

Given BER and ABEL, we can now estimate the mean time between burst errors (MBE) which represents the reciprocal of the average frequency of the burst error. As Channel SNR goes up, ABEL becomes smaller and MBE becomes longer. Table 1 shows the Channel errors for several different Channel SNRs at the same bit rate. In Table 1, the MBE is calculated as that given in [15].

$$MBE = \frac{ABEL}{BER \times 1.152(Mbps)} \tag{11}$$

From Table 1, it is seen that in the case of Channel SNR = 10 or 15 dB, the ABEL exceeds the size of the signal frame. Therefore, in these cases, some of the neighboring frames are also corrupted. For simplicity, it is assumed that a whole frame is lost even when a small portion of the frame is corrupted.

Table 1. Channel error estimation at 1.152 Mbps

Channel SNR (dB)	ABEL	BER	MBE (Frames, 10ms)
10	24995.5	0.036	60.8
15	13891.8	0.011	106.8
20	7782.2	0.0036	189.2
25	4370.9	0.00113	336
30	2457	0.000357	597.2
35	1381	0.000113	1061.8
40	776.9	$(3.57) 10^{-5}$	1888.2
50	245.7	$(3.57) 10^{-6}$	5970.8

PC-AMBTC Algorithm

The image is decomposed into a number of subbands using Pyramid Coding (PC). Each of these subbands is called a level. Let $x_0(n_1,n_2)$ denote the original image as shown in Fig. 2. We will refer to $x_0(n_1,n_2)$ as the base level image of the Pyramid. The image at one level above the base is obtained by low-pass filtering $x_0(n_1,n_2)$ and then subsampling (decimating) the result by 4:1. The result of the decimation operation can be denoted by the image $x_1(n_1,n_2)$, which is smaller in size than $x_0(n_1,n_2)$ by a factor of sixteen due to the decimation operation. The image $x_1(n_1,n_2)$ is the first-level image of the Pyramid. The second level image, $x_2(n_1,n_2)$, is obtained by lowpass filtering of the first-level image $x_1(n_1,n_2)$ and then decimating the result by 4:1. This procedure can be repeated to generate a higher level image. To encode the original image $x_0(n_1,n_2)$, we encode $x_1(n_1,n_2)$ and the difference between $x_0(n_1,n_2)$ and the prediction of $x_0(n_1,n_2)$ from $x_1(n_1,n_2)$.

The image will be encoded using the algorithm shown in Fig. 2. The original image $x_0(n_1,n_2)$ is decomposed into two images $x_1(n_1,n_2)$ and $c_0(n_1,n_2)$ using one level Pyramid coding [16]. The decimated image $x_1(n_1,n_2)$ encoded by using absolute

moment block truncation coding (AMBTC) with a block size of 4 x 4 pixels each [17]. Then, the encoded image $\hat{x}_1(n_1,n_2)$ is synthesized to produce the image $y_1(n_1,n_2)$ with the same size as the original image $x_0(n_1,n_2)$. The difference image $e_0(n_1,n_2)$ is encoded by using the concept of geometric vector quantization (GVQ) proposed in [18]. However, the GVQ is modified for farther compression as will be discussed in the following section.
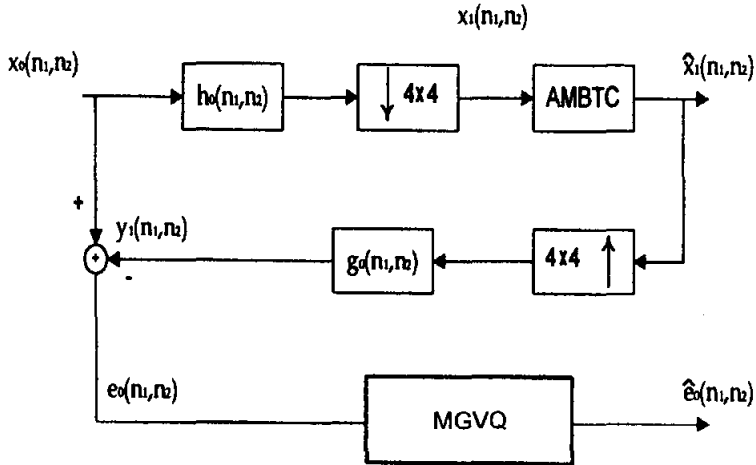

Fig. 2. The one-level encoder with AMBTC and MGVQ.

Modified GVQ for the Difference Image

The difference image $e_0(n_1,n_2)$ contains the high frequency information (edge information) and the decoded error results from decoding the low frequency band $x_1(n_1,n_2)$. Although this information is low in energy content, the difference image (high frequency band) contains information that effects the visual quality of the encoded image. Therefore, an efficient coding algorithm is desired. This algorithm should preserve the edge geometrics and follow the energy variation of the local blocks. Those blocks with high energy will be efficiently transmitted and those with low energy will be transmitted with low bit rate. In this paper, the method of GVQ proposed by C. I. Podilchuke and N. S. Jayant in [18] is modified as follows:

1. The block dimension is selected to be 8x8 or 4x4.
2. The threshold for edge detection is adaptive and depends on the amount of energy in each block.

3. Local adaptive vector quantization (LAVQ) as proposed in [19] is used for the high and low mean transmission of GVQ.
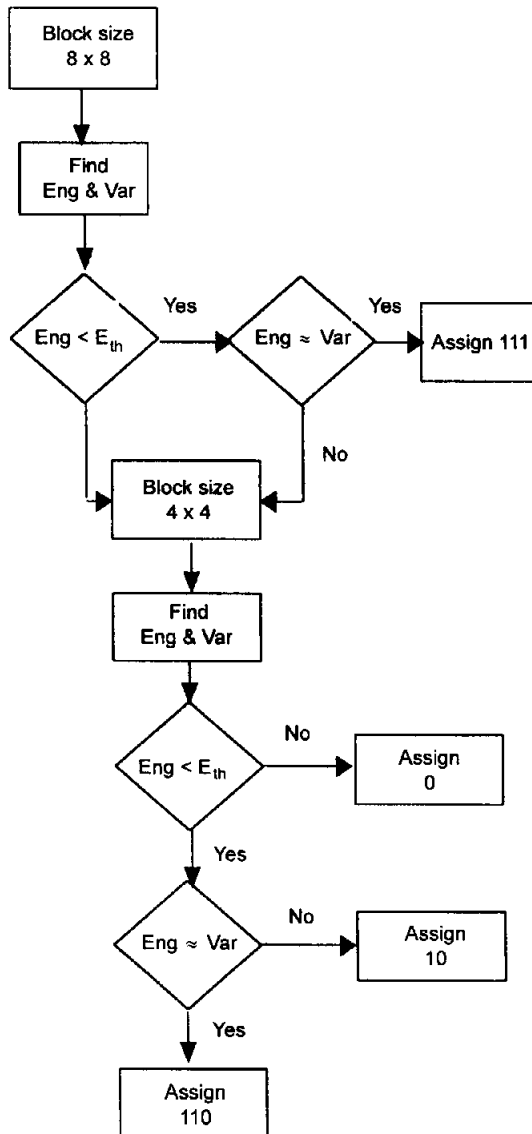4. The overall algorithm (MGVQ) is processed as shown in Fig. 3.

Fig. 3. The modified GVQ.

An 8x8 block is selected from the difference image first. Then, the energy and variance of this block are calculated. As shown in Fig. 3, if the energy (Eng) is less than or equal to the energy threshold (E_{th}), then, the variance will be compared with the energy and if the difference is very less then send ``111`` followed by the mean of that block. For the calculation of the high mean and low mean, the concept of GVQ is adapted. However, the mean which represents more pixels of the block will be transmitted at rate of 8 bits. A high compression is achieved since instead of transmitting 512 bits (8 bits for each of the 64 pixels) for this block, only 11 bits are transmited (8 bits for mean and 3 bit for over head). If any of the conditions fails, then the method proposed in Fig. 3 is adapted.

The LAVQ codebook size is 127 codewords each 2 pixels (high mean and low mean). This VQ technique is used only when the overhead codeword is assigned ``0``. The bit map in this case is sent as it is.

When the overhead codeword is "10", the same concept that is adapted for the codeword "111" is applied. However the compression achieved in this case is lower since we transmit 10 bits (8 bits for mean and 2 for overhead) instead of 128 bits (8 bits for each of the 16 pixels). If the overhead codeword is "110", the block of size 4x4 will not be transmitted and at the receiver all the values of the 16 pixels will be assigned zeros. This algorithm will give long runs of zeros, which make this algorithm suitable for run length coding (RLC). Therefore, the adaptation of RLC could be investigated. The visual quality is excellent at low bit rate.

The symbols used in Fig. 3 are defined below:
Eng = Block energy
Var = Block variance
E_{th} = Energy threshold
0   = Send the 4x4 block using GVQ
10   = Send the mean H_m or L_m for 8x8 block
110 = No transmission
111 = Send the mean (H_m or L_m) for 4x4 block
H_m = High mean
L_m = Low mean
$\approx$ = Approximately equal

Simulation Results

In this paper, we will simulate our algorithm for two images. The "ksu-boy2" image of dimension 256 x 256 with 8 bpp and the standard image called "Lena" of 512 x 512 dimension with 8 bpp. Only the bit rate and SNR for Lena will be presented for the sake of comparison with the existing algorithms. The visual quality of this image is found to be acceptable. For the ksu-boy2 image, we will display the reconstructed images and test their visual quality at different Channel SNR (dB).

Figure 4 shows the original image for ksu-boy2. The image is first decomposed into two images. Namely, the base-band (decimated image) and the high-band (difference image). Fig. 5 shows the reconstructed image at the receiver without Channel error at rate of 0.31 bpp and PSNR= 34.41 dB.

Fig. 4. The original (ksu-boy2) image.

Fig. 5. The reconstructed (ksu-boy2) image (without channel error) at rate of 0.31 bpp and PSNR=34.41 dB.

We assume that a whole frame is lost even when a small portion of the frame is corrupted. Fig. 6 shows the reconstructed images when one or three error frames accrued in the encoded (decimated) image which has most of the information about the original image. The simulation results for the peak signal -to- noise ratio (PSNR) and mean square reconstructed error (MSE), with variation of frames in error between the decimated and the difference images for the ksu-boy2 image are given in Tables 2 and 3; respectively. From these Tables, it is seen that the encoded decimated image have large effect on the values of PSNR since each bit of this band contains a significant amount of information about the original image. Therefore, this band will be protected from Channel fading errors by using error correction code techniques. The increasing in the bit rate as result of Channel coding is very small. While, the encoded difference image has small effect on the overall reconstructed image.

(a)

(b)

Fig. 6. Reconstructed (ksu-boy2) image with, (a) one error frame; (b) three errors frame. (all errors frame are in the encoded decimated image).

To compare our algorithm with other existing algorithms, the standard image called "Lena" is simulated for Channel SNR between 10 and 35 dB. Figure 7 shows plots of the average peak SNR performances when fading errors occurred at different locations of data stream. In this Figure, curve 1 denote the average PSNR versus Channel SNR for the case when Channel fading occurs only in the encoded difference image. Curve 3 represents the average PSNR values when fading errors occur only in the encoded decimated image. Curve 2 is the average plot denotes the average PSNR for the evenly distributed fading errors over the entire data stream. From curve 1 of Fig. 7, it is clear that the errors in the encoded difference image have very little effect on the average PSNR value. From curve 3 the errors in the encoded decimated image have large effect on the average PSNR value because it has most of the signal power of the original image.
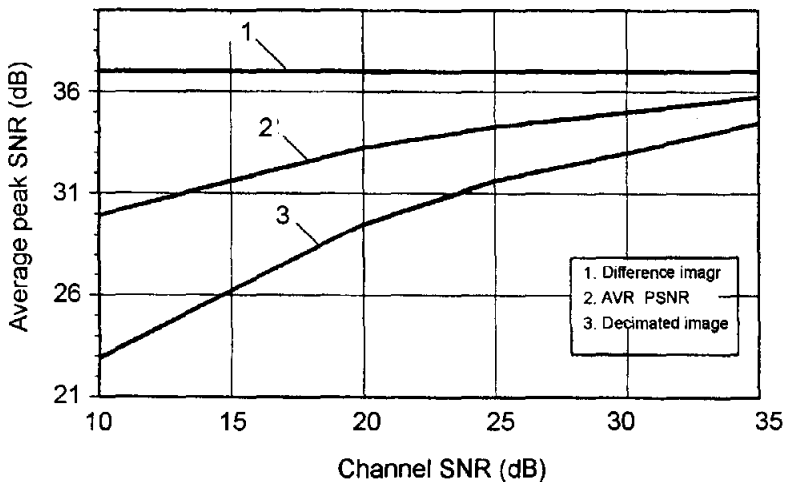

Fig. 7. Transmission performance for "Lena" image using PC-AMBTC algorithm.

Table 2. The MSE and PSNR with variation frame errors for the "ksu-boy2" in the encoded decimated image

No. of frames error for (x_1)	MSE	PSNR (dB)
0	13.8	36.73
1	67.35	29.85
2	237.8	24.37
3	275.7	23.72

Table 3. The MSE and PSNR with variation frame errors for the "ksu-boy2" in the encoded difference image

No. of frames error for (e_0)	MSE	PSNR (dB)
0	13.8	36.73
1	55.93	31.95
2	218.3	30.4
3	247.2	29.88

Performance Evaluation

The proposed algorithm (PC-AMBTC) is simulated and compared with other existing algorithms such as the subband multistage vector quantization (SB-MSVQ) coding proposed by E.S. Jang and N.M. Nasrabadi in [9]. In that paper, they have compared themselves with the standard algorithm JPEG and found that the (SB-MSVQ) performed better than the baseline JPEG standard. They demonstrate that the "Lena" image can be encoded at bit rate of 0.69 bit per pixel (bpp) at peak signal-to-noise ratio (SNR) = 39.3 dB. The JPEG at the same SNR will compress the image at rate of 0.57 bpp. However, the bit rate of the encoded image using JPEG (after packetization) will be 0.73 bpp. They found out that the increase in the bit rate is due to the structure of the JPEG data stream [9].

A.   Comparison with SB-MSVQ and JPEG

To compare the performance of the proposed algorithm (PC-AMBTC) with SB-MSVQ coding and baseline JPEG algorithms, we can do this by comparing the average PSNR (curve 2 of Fig. 7) with the simulation results given in [9]. This comparison is shown in Fig. 8. From this figure, it is found that the overall average peak SNR of PC-AMBTC is higher than the SB-MSVQ and baseline JPEG at the same bit rate.

1). *Qualitative evaluation*: The visual quality of the reconstructed image is excellent in PC-AMBTC algorithm. It is almost indiscernible from the original image in absence of fading.

2). *Quantitative evaluation*: The performance of the proposed algorithm is compared based on the signal to noise ratio, bits per pixel requirements, and computational complexity.

I) *PSNR and BPP Requirements:* The improvement of the PSNR of the proposed algorithm over the SB-MSVQ and JPEG algorithms is given in Table 4. The improvement over SB-MSVQ is increasing as the Channel SNR increased. However, the PC-AMBTC technique gives an increase in the PSNR with an average of 2 dB over the standard JPEG algorithm at any Channel SNR as shown in Table 4. Therefore, the performance of PC-AMBTC algorithm is better than the existing algorithms at any Channel SNR at the same bit rate (bpp).

II) *Computational complexity:* The proposed technique is lower in complexity than these algorithms. The SB-MSVQ combines the subband coding technique with the multistage vector quantization. This will make the encoder/decoder of high complexity. Also, the JPEG used the discrete cosine transform concept which made the encoder/decoder of high complexity. However, the PC-AMBTC is only one level Pyramid encoder that decomposed the original image into two images. These images are encoded with the very simple encoder techniques called AMBTC. For the decimated image the AMBTC is used directly at 2 bpp. For the difference image, the AMBTC is used in form of vector quantization with a very simple design codebook as described in the previous section. Overall, the PC-AMBTC compression algorithm is found to be of lower complexity than the existing techniques.

Table 4. The PSNR (dB) improvement of PC-AMBTC over SB-MSVQ and JPEG algorithms for different Channel SNR at the same (bpp)

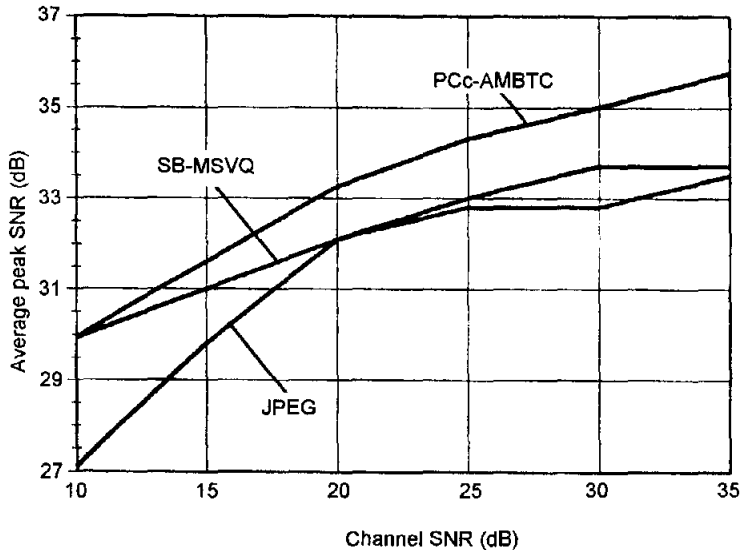| Channel SNR (dB)	10	15	20	25	30	35
PSNR improvement over JPEG (dB)	2.82	1.90	1.30	1.50	2.20	2.50
PSNR improvement over SB-MSVQ (dB)	0	0.70	1.30	1.30	1.30	2.30

Fig. 8. Performance comparison of PC-AMBTC algorithm with SB-MSVQ and baseline JPEG algorithms for the standard "Lena" image.

Conclusion

The proposed algorithm for image coding over a fading Channel gives an acceptable image quality at very low bit rate. The performance of the PC-AMBTC is compared with the performance of the SB-MSVQ and the baseline JPEG. Simulation results show that the proposed PC-AMBTC is very robust to Channel fading errors in a DECT environment. The baseband (decimated image) contains the most important part of the data stream. Therefore, this band has to be protected against the error caused by fading Channels.

The PC-AMBCT technique is lower in complexity than SB-MSVQ and the baseline JPEG. It is considered to be of low complexity encoder/decoder. The GVQ is modified for the difference image. Applying variable length code for the overhead and LAVQ indices could reduce the bit rate for this band. Our current research regarding the compression of the data is to design a lossless code for the overhead codeword and the indices of the codebook.

References

[1]   Fletcher, P. "DECT-standard Demo Puts Full-motion Video Over Cordless-telephone Link." *Electron. Design,* 40 (Sept. 1992), 34.

[2]   Stedman, R., Gharavi, H., Hanzo, L. and Steele, R. "Transmission of Subband-coded Image via Mobile Channels." *IEEE Trans. on Circuits Syst. Video Technol,* 3 (Feb. 1993), 15-26.

[3]   Lops, L.B. "Performance of the DECT System in Fading Dispersive Channels." *Electron. lett.,* 26 (Aug. 1990), 1416-1417.

[4]   Sayood, K. *Introduction to Data Compression.,* Morgan Kaufmann Publishers, Inc., 1996.

[5]   Clark, R.J. *Digital Compression of Still Images and Video.,* Academic Press, Inc., 1995.

[6]   Metin, K., Vetterli, M. and Legall, D.J. "Interpolative Multiresolution Coding of ATV with Compatible Sub-channels." *IEEE Trans. on Circuits and Syst. Video Technol.* 1, No. 1(March 1991), 89-99.

[7]   Al-Asmari, A.Kh., Singh, V.J. and Kwatra, S.C. Hybrid Coding of Images for Progressive Transmission over a Digital Cellular Channel." *In Proc. IEEE Int. Conf. on Imaging Science, Systems, and Technology,* Las Vegas, Nevada: Monte Carlo Resort., (June 28 – July 1, 1999), 120-125.

[8]   Zhang, Y., Liu, Y. and Pickholtz, R.L. "Layered Image Transmission over Cellular Radio Channels." *IEEE Trans. on Veh. Technol.,* 43, No. 3 (Aug. 1994), 786-794.

[9]   Jang, E.S. and Nasrabadi, N.M. "Subband Coding Multistage VQ for Wireless Image Communication." *IEEE Trans. on Circuits Syst. Video Technol,* 5, No. 3 (June. 1995), 247-253.

[10]   Al-Asmari, A.Kh. "Multiresolution Image Coding for Wireless Channel." In: *Proc. IEEE Int. Conf. on Consumer Electronics,* Los Angeles: California, (June 1998), 38-39.

[11]   Howell, E.I.F. "DECT Beyond CT2." *IEE Rev.,* 38 (July/Aug. 1992), 263-268.

[12]   Goodman, D.J. "Second Generation Wireless Information Networks." *IEEE Trans. Veh. on Technol.,* 40 (May 1991), 365-374.

[13]   Garg, V.K. and Wilkes, J.E. *Wireless and Personal Communications Systems.,* Prentice Hall, Inc., 1996.

[14]   Murota, K. and Hirade, K. "GMSK Modulation for Digital Mobile Radio Telephony." *IEEE Trans. on Commun.,* 29 (July 1981), 1044-1050.

[15]   Otani, K. and Omori, H. "Distribution of Burst Error Lengths in Rayleigh Fading Radio Channels." *Electron. Lett.,* 16 (Nov. 1980), 889-891.

[16]   Al-Asmari, A.Kh. "Optimum Bit Rate Pyramid Coding with Low Computational and Memory Requirements." *IEEE Trans. on Circuits Syst. Video Technol.,* 5, No. 3 (June 1995), 182-192.

[17]   Lemma, M.D. and Mitchell, O.R. "Absolute Moment Block Tuncation Coding and Its Application to Color Image." *IEEE Trans. on Commun.*, 32, No. 10 (Oct. 1984), 1148-1157.

[18]   Podilchik, C., Jayant, N. and Farvardin, N. "Three Dimensional Subband Coding of Video." *IEEE Trans. on Image Processing.*, 4, No. 2 (Feb. 1995), 125-138.

[19]   Al-Asmari, A.Kh. and Ahmed, A.S. "A Low Bit Rate Hybrid Coding Scheme for Progressive Image Transmission." *IEEE Trans. on Consumer Electronics*, 44 (Feb. 1998), 226-234.

خوارزم منخفض التعقيد لإرسال الصور المضغوطة عبر قناة اتصال لاسلكية

عوض خزيم الأسمري

قسم الهندسة الكهربائية ، كلية الهندسة ، جامعة الملك سعود ، ص. ب. ٨٠٠ ،
الرياض ١١٤٢١ ، المملكة العربية السعودية

ملخص البحث. تم في هذه الورقة اقتراح التشفير الهرمي و طريقة العزم المطلق لترميز الكتل المبتورة PC-) (AMBTC لإرسال الصور عبر قناة اتصال لاسلكية. استُخدم جهاز الاتصال الرقمي اللاسلكي الأوروبي والمعروف ب (DECT) كوسيط (قناة) اتصال لاسلكي. تم في هذه الدراسة بحث تأثير خَبْو (fading) القناة على خوارزم (PC-AMBTC) ومن ثم مقارنة كفاءته مع خوارزميات أخرى.

تم تقسيم الصورة الأصلية إلى صورتين (الصورة المختزلة و صورة الفرق) باستخدام مرشح ذو نطاق منخفض. أستُخدِمت طريقة (AMBTC) في ترميز الصورة المختزلة بينما أستُخدِم تكمية المتجه الهندسي المعدّل (MGVQ) لترميز صورة الفرق. وبما أن معظم الطاقة و المعلومات مركّز في نطاق الصورة المنخفض التردد (صورة الفرق) ، فإنه يجب حماية المعلومات في هذا النطاق من تأثير الخطأ الحادث من خَبْو (fading) القناة.

أثبتت نتائج المحاكاة بأن الخوارزم المقترح في هذه الورقة قوي ضد الأخطاء الناجمة عن خبو القناة. وكذلك وجد أنه أعلى كفاءة من الطرق المستخدمة حالياً عند نفس معدّل الإرسال.